УДК 004:528

АВТОМАТИЗОВАНЕ ВИЯВЛЕННЯ ТА ОЦІНКА СПРИЧИНЕНИХ ВІЙНОЮ ПОШКОДЖЕНЬ СІЛЬСЬКОГОСПОДАРСЬКИХ ПОЛІВ ЗА ДОПОМОГОЮ СУПУТНИКОВИХ ЗОБРАЖЕНЬ

AUTOMATED DETECTION AND ASSESSMENT OF WAR-INDUCED DAMAGE TO AGRICULTURAL FIELDS USING SATELLITE IMAGERY

Куссуль Н., Дрозд С., Яйлимова Г.
Kussul N., Drozd S., Yailymova H.
National Technical University of Ukraine "Igor Sikorsky Kyiv Polytechnic Institute", Kyiv, Ukraine
Space Research Institute of the National Academy of Sciences of Ukraine and the National Space Agency, Kyiv, Ukraine
ORCID: https://orcid.org/0000-0002-9704-9702, https://orcid.org/0000-0002-5149-5520,
https://orcid.org/0000-0001-6116-8294
E-mail: kussul.nataliia@gmail.com, sofi.drozd.13@gmail.com, anna.yailymova@gmail.com

DOI:

Abstract. *This paper introduces a methodology based on machine learning and remote sensing for detecting military-induced damages to agricultural lands in Ukraine using free Sentinel-2 satellite data. The most informative spectral bands (B2, B3) and vegetation indices (NDVI, GCI) were experimentally selected for recognizing damaged fields through the Random Forest classification algorithm. Additionally, an anomaly detection method based on the estimation of deviations of pixel values from the mean within each field was applied to determine local damage in the identified affected fields. The proposed methodology demonstrated high classification accuracy with an f1-score of 0.87%, producer’s accuracy of 0.89%, user’s accuracy of 0.85, and sensitivity for detecting local damage. The developed anomaly detection method allows to recognize damage visible on the 10-meter pixel of the Sentinel-2 satellite, but does not identify small craters. Cloudiness of satellite images can significantly impair the accuracy of damage detection, and the method of local damage detection can respond to non-military anomalies and requires careful selection of threshold coefficients for each field. The study conducted a comprehensive assessment of damages inflicted on Ukrainian agricultural fields during the period 2022-2023, revealing that a total of 1,544,952 hectares, equivalent to 5.72% of the total agricultural area, experienced damage. This included 509,107 ha of wheat, 114,302 ha of sunflower, 68,830 ha of maize, 4,029 ha of rapeseed, and 16,561 ha of other crops. The most affected regions were Donetsk, Zaporizhia, and Kherson oblasts. The comprehensive findings of this research provide valuable insights for monitoring the state of agriculture and formulating strategic plans for the recovery of agricultural resources amidst the ongoing military conflict.*

Анотація*. Ця стаття представляє методологію, засновану на машинному навчанні та дистанційному зондуванні для виявлення збитків, спричинених військовими діями, сільськогосподарським землям в Україні за допомогою безкоштовних супутникових даних Sentinel-2. Експериментально відібрано найбільш інформативні спектральні смуги (B2, B3) та індекси рослинності (NDVI, GCI) для розпізнавання пошкоджених полів за допомогою алгоритму класифікації Random Forest. Крім того, метод виявлення аномалій, заснований на оцінці відхилень значень пікселів від середнього в кожному полі, був застосований для визначення локального пошкодження в ідентифікованих уражених областях. Запропонована методологія продемонструвала високу точність класифікації з показником f1 0,87%, точністю виробника 0,89%, точністю користувача 0,85 і чутливістю для виявлення локальних пошкоджень. Розроблений метод виявлення аномалій дозволяє розпізнати пошкодження, видимі на 10-метровому пікселі супутника Sentinel-2, але не ідентифікує невеликі кратери. Помутніння супутникових знімків може значно погіршити точність виявлення пошкоджень, а метод виявлення локальних пошкоджень може реагувати на невійськові аномалії та вимагає ретельного підбору порогових коефіцієнтів для кожного поля. Дослідження провело комплексну оцінку збитків, завданих сільськогосподарським полям України протягом 2022-2023 років, виявивши, що загалом пошкоджено 1 544 952*

га, що еквівалентно 5,72% від загальної сільськогосподарської площі. З них 509 107 га пшениці, 114 302 га соняшнику, 68 830 га кукурудзи, 4 029 га ріпаку та 16 561 га інших культур. Найбільше постраждали Донецька, Запорізька та Херсонська області. Комплексні результати цього дослідження дають цінну інформацію для моніторингу стану сільського господарства та формулювання стратегічних планів відновлення сільськогосподарських ресурсів в умовах триваючого військового конфлікту.

Keywords: machine learning, classification, anomaly detection, satellite data, Sentinel-2, war damaged fields, spectral bands, vegetation indices.

Ключові слова: машинне навчання, класифікація, виявлення аномалій, супутникові дані, Sentinel-2, пошкоджені війною поля, спектральні смуги, індекси рослинності.

1. Introduction

Ukraine is one of the world's largest exporters of agricultural products, but its agriculture has suffered significant damages [1, 2] due to the full-scale invasion by Russia, which commenced on February 24, 2022. As reported by the Kyiv School of Economics [3], as of February 24, 2023, the losses in Ukraine's agrarian sector are estimated at 40.2 billion US dollars. Thousands of hectares of fields are mined, shelled, burned, or simply inaccessible for cultivation due to occupation. This has posed significant challenges for the cultivation of agricultural crops and logistics, and it threatens food security not only in Ukraine but also globally.

For the effective restoration of damaged agricultural lands and ensuring food security, accurate information about the location and condition of the affected areas is crucial. However, local assessment is challenging and dangerous due to occupation, ongoing conflict, or unexploded ordnance. Therefore, an automated algorithm is needed to remotely detect damaged territories, for example, using satellite data.

Satellite data provides almost real-time monitoring and offers not only spectral images for visual interpretation but also valuable information on plant vegetation, soil surface temperature, moisture, etc., beneficial for predicting crop yields [4-6], detecting droughts [7-9], floods [10], or plant damage from hailstorms [11, 12]. High spatial resolution and frequent updates, such as daily data from MAXAR or WorldView-2 [13], are most suitable for detecting war-induced damages to agricultural fields. However, these commercial images are expensive, limiting their use for continuous monitoring over large areas. In contrast, open and free sources like Sentinel-2, with a spatial resolution of 10 meters and an update frequency of 5 days, can be utilized. Combining Sentinel-2 images with advanced machine learning technologies allows the development of an efficient algorithm for monitoring crops and land degradation [14], detecting fires [15, 16], or other military-induced damages to agricultural fields [17, 18].

The development of an automated algorithm based on satellite data and machine learning for remote recognition of military-induced damages to fields will assist the government of Ukraine and international organizations in responding promptly and accurately to crisis situations and planning recovery measures. This algorithm can be valuable not only for Ukraine but also for other countries facing similar conflicts on their territories.

2. Literature Analysis and Problem Statement

Over the past years, many researchers and experts in the fields of agriculture and geoinformatics have devoted significant attention to developing methods for assessing war-induced damages to agricultural fields and determining effective means of remote detection. This research trend reflects an understanding of the need for advanced technological tools to identify and evaluate damages, which can be applied for crisis response and agricultural infrastructure recovery planning.

For assessing damage to the agricultural sector resulting from the 1992-1995 war in northeastern Bosnia, scientists conducted a study [19] on detecting abandoned agricultural lands using multi-temporal Landsat TM images. Controlled classification of Landsat TM data identified abandoned agricultural lands with an overall accuracy of 82.5%. A similar study [20] on land use changes due to war was conducted in Iraq. Scientists used MODIS NDVI and Landsat NDVI data to study changes in cultivated areas over three decades from 1990. Satellite data helped identify the dates and locations of abandoned lands, as well as changes in cultivated areas.

Eklund et al. [21] assessed the impact of war on land use changes in the territories captured by the Islamic State since 2014 in Syria and Iraq, using time series of 250-meter MODIS data and a random forest classifier to identify land cover classes. Similar assessments were conducted directly for the territory of Ukraine. Kostyuchenko et al. [22] proposed an adaptive Markov chain method for studying land use changes in the Donbas region (Eastern Ukraine) during the conflict in 2014-2015 using Landsat and MODIS satellite data. Skakun et al. [23] analyzed changes in eastern Ukraine from 2014 to 2019 using Landsat and Sentinel data. Deininger et al. [2] conducted an econometric analysis of the impact of the 2022 Russian war on winter crop production in Ukraine.

While these methods have been useful for a global assessment of the impact of military conflicts on agricultural land degradation, their limitation lies in tracking changes in land use without assessing the degree of damage or providing accurate location information for affected areas.

In contrast, Lin et al. [13] focused on identifying craters and searching for unexploded ordnance in fields affected by the Vietnam War in Cambodia, using commercial multispectral WorldView-2 images and a two-stage machine learning structure. The developed algorithm increased detection by over 160% compared to its predecessors, revealing that up to 50% of unexploded ordnance in fields remained a danger. Lacroix and Vanhuysse [24] also focused on crater identification in Cambodia based on panchromatic satellite images obtained by Pleiades 1A and the "Constrained Gradient for Circle" (CGC) method. Duncan et al. [25] conducted a similar analysis for detecting artillery craters in Ukrainian agricultural fields that occurred during the armed conflict in 2014, using WorldView-2 images and deep learning methods. The accuracy of the

developed U-Net model depended on the crater size, with an F-score of 0.80 for craters >60 m².

These studies provide data on localization, the number of craters, their characteristics such as diameter, and even allow determining the type of weaponry that caused the damages in fields. However, these studies require the use of commercial satellite data and were conducted over small territories within a fixed time period.

For the analysis of large territories and long-term observations, Kussul et al. [17] used a free alternative – Sentinel-2 satellite images and applied a change detection method. The scientists compared NDVI calculated from two temporally adjacent satellite images to detect damages in fields. Another Sentinel-2-based approach [18] involved applying an anomaly detection method in the blue and green spectral bands.

However, these methods have limitations as they react not only to war-induced damages but also to natural changes in fields. To address this limitation, the incorporation of machine learning methods, particularly classifiers, and the combination of different vegetation indices and spectral bands are planned in our research.

3. Object, Subject, and Aim of Research

The ***aim*** of this research is to develop an algorithm for the automatic detection of war-induced damages in fields based on free satellite images and machine learning. This algorithm is designed to be applicable to large territories and for long-term observations.

The ***subject*** of this study is the agricultural fields in eastern Ukraine.

The ***object*** of the research is the process of identifying damages on agricultural fields using satellite images and machine learning.

As the ***study area*** (Fig. 1), we selected 10 regions in eastern and southern Ukraine where the armed conflict is most active, according to data from the Armed Conflict Location & Event Data Project [26]. These regions include Kyiv, Chernihiv, Summy, Kharkiv, Donetsk, Luhansk, Zaporizhia, Dnipropetrovsk, Kherson, and Mykolaiv.

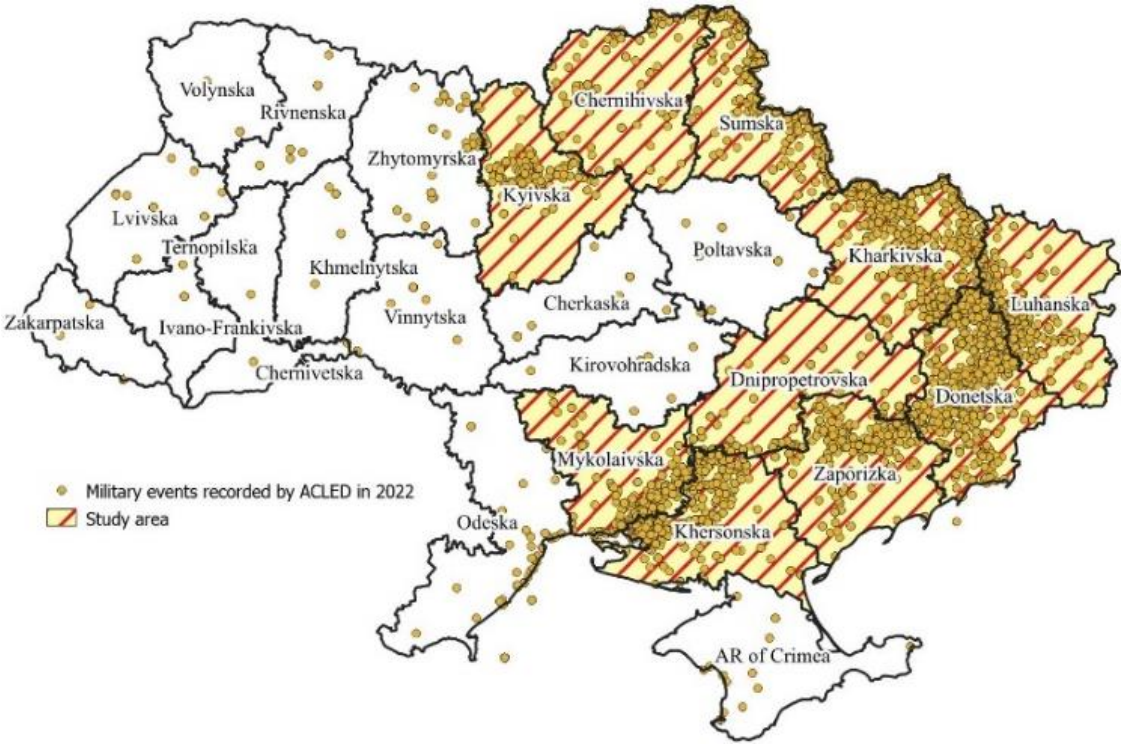

Fig. 1. Study area

To conduct our research, we employ the cloud-based infrastructure of Google Earth Engine (GEE) because it provides fast access to satellite data and powerful computational resources for processing, including machine learning tools.

Our primary data source consists of bi-weekly composites from the Sentinel-2 satellite, which have been pre-processed to remove cloud cover and overlaid with a mask depicting agricultural crops based on a classification map [27]. To analyze information at the field level, we utilize field delineation data for the year 2022, generated by the Sinergise company as part of the EO4UA initiative [28].

4. Methodology

In this study, we propose a three-step methodology (Fig. 2):

1. ***Manual identification of damaged fields*** through photo interpretation of images to collect training data for machine learning.
2. ***Classification*** to recognize damaged fields among all agricultural lands (subsection 3.2.2).
3. ***Anomaly detection*** to identify local damages and assess their severity within each classified damaged field (subsection 3.2.3).

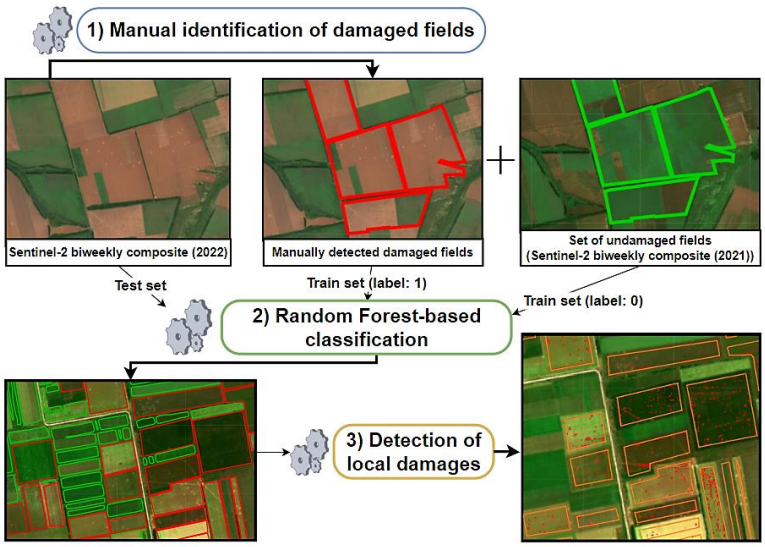

Fig. 2. Damage detection algorithm

4.1. Selection of the most informative parameters for machine learning

The Sentinel-2 satellite, whose data we use in our study, has eight spectral bands with a resolution of 10-30 m. To develop an effective algorithm for detecting damages to agricultural fields, it is crucial to select only the most informative data. We decided to focus solely on the data from the 10-m bands, including B2 (blue), B3 (green), B4 (red), and B8 (near-infrared), as well as vegetation indices that are combinations of these bands – NDVI (Normalized Difference Vegetation Index), GCI (Green Chlorophyll Index), AVI (Atmospherically Resistant Vegetation Index), and EVI (Enhanced Vegetation Index).

During the examination of satellite imagery in the RGB (Red-Blue-Green) spectrum, we observed that explosions and military vehicle movements damage vegetation and disrupt the topsoil layer. In fields with low vegetation, subsurface exposure occurs. Therefore, we assume that in certain bands and vegetation indices, pixel values corresponding to damaged areas will significantly differ from the average pixel values within the field. To test our hypothesis and identify which spectral bands and vegetation indices are most sensitive to damages, we analyze the distribution of pixel values of spectral and vegetation indices within fields before and after damage. For this purpose, we selected three types of fields - undamaged, moderately damaged, and heavily damaged (Fig. 3), which were planted with the same crop (wheat), located close to each other, had approximately the same area, and were in a similar stage of vegetation.

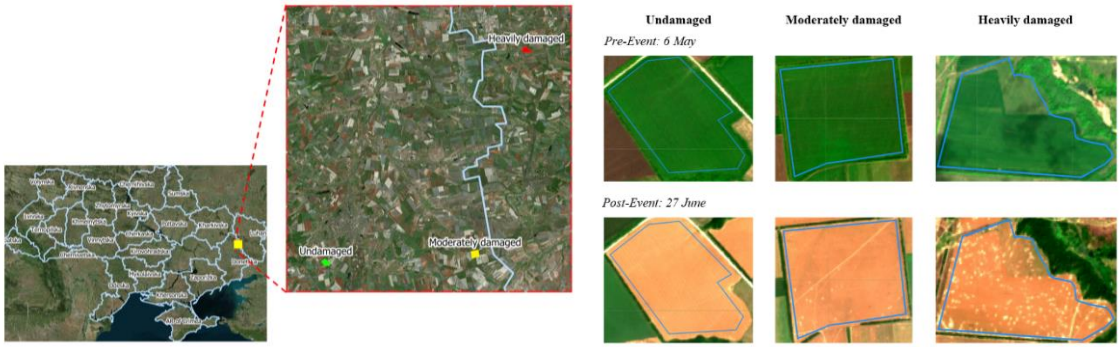

Fig. 3. Fields before and after damage

From the density plots in Fig. 4a, it is evident that after potential damage, the values of spectral bands B2 and B3 decreased for moderately and severely damaged fields compared to undamaged ones. A pronounced decrease in band values is observed for the severely damaged field, even with higher initial values. For bands B4 and B8, the differences are less pronounced: the distribution of values for B4 between damaged and undamaged areas shows no significant difference, and for B8, the differences between damage levels are not substantial. In Fig. 4b, vegetation index plots show almost identical NDVI values before the event. After damage, a reduction in NDVI is observed for damaged fields, especially pronounced in cases of severe damage. EVI and AVI indices respond similarly to NDVI. The GCI index responds to damage similarly to band B8 – a moderately damaged field has the most significant left shift (i.e., a decrease in index values). However, for severely damaged fields, a notable tail in the distribution, directed to the left, can be observed.

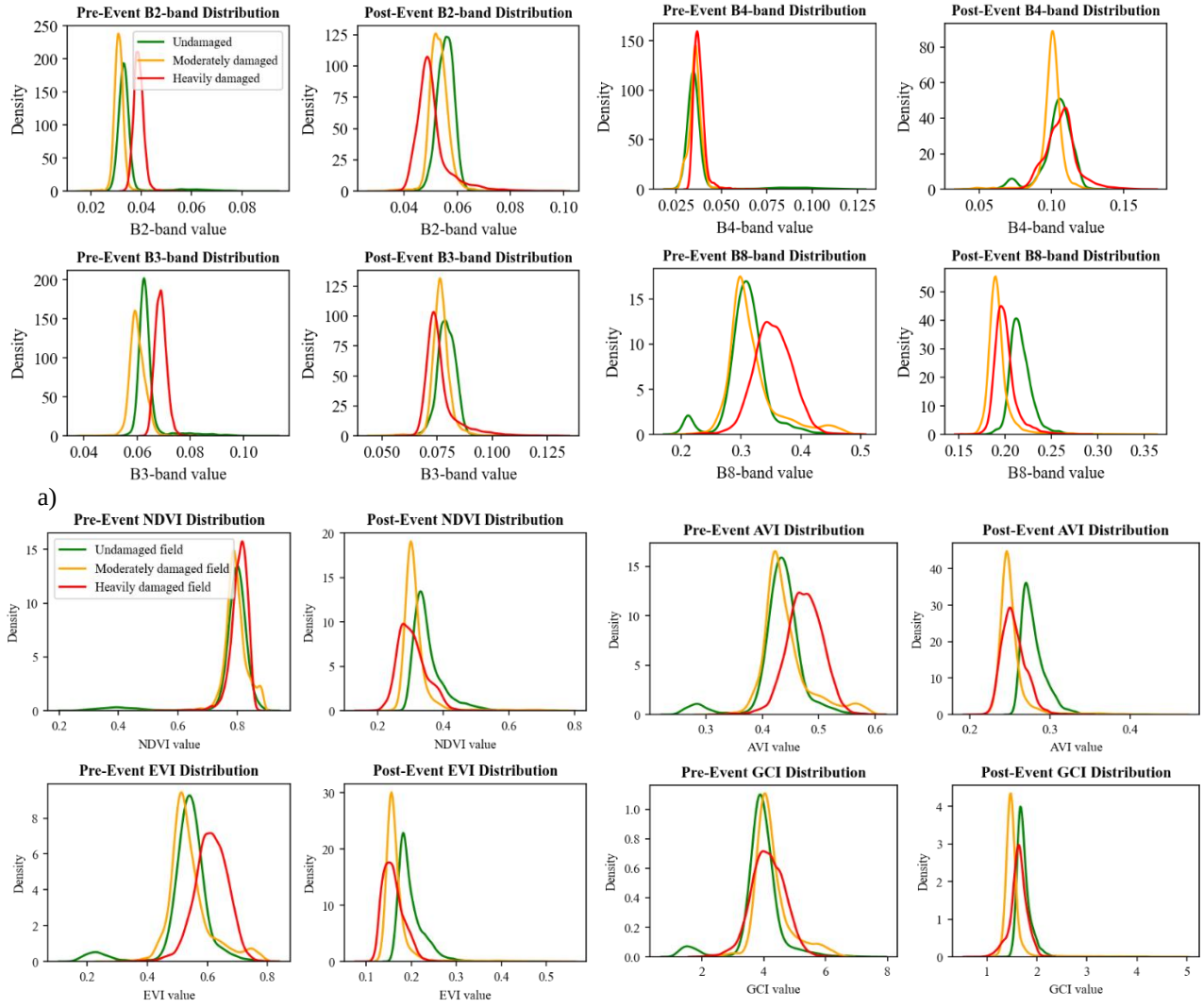

Fig. 4. Examples of a shift in the distribution of pixels values: a - spectral bands, b - vegetation indices

To better understand how specific spectral bands and vegetation indices respond to damage, we conducted another experiment in which we attempt to distinguish normal and anomalous pixel values by their deviation from the mean value within the field using formula 1:

$$Band_{damaged} = \begin{cases} 1, Band_{mean} - Band < 2 * Band_{std} \\ 0, Band_{mean} - Band \geq 2 * Band_{std} \end{cases} \quad (1)$$

In this formula, Band - is the pixel values of a specific band, $Band_{mean}$ - is the mean pixel value of band within the field, $Band_{std}$ - is the standard deviation of pixel values for a specific band within the field, and $Band_{damaged}$ - is a pixel with an anomalous value. We use a threshold value of two standard deviations to detect anomalies, as approximately 95% of data in a normal distribution falls within this range from the mean [29].

For vegetation indices, we apply a similar formula. However, unlike spectral bands where we also anticipated possible increases in values, for vegetation indices, we only subtract two standard deviations, anticipating a decrease in vegetation on damaged areas.

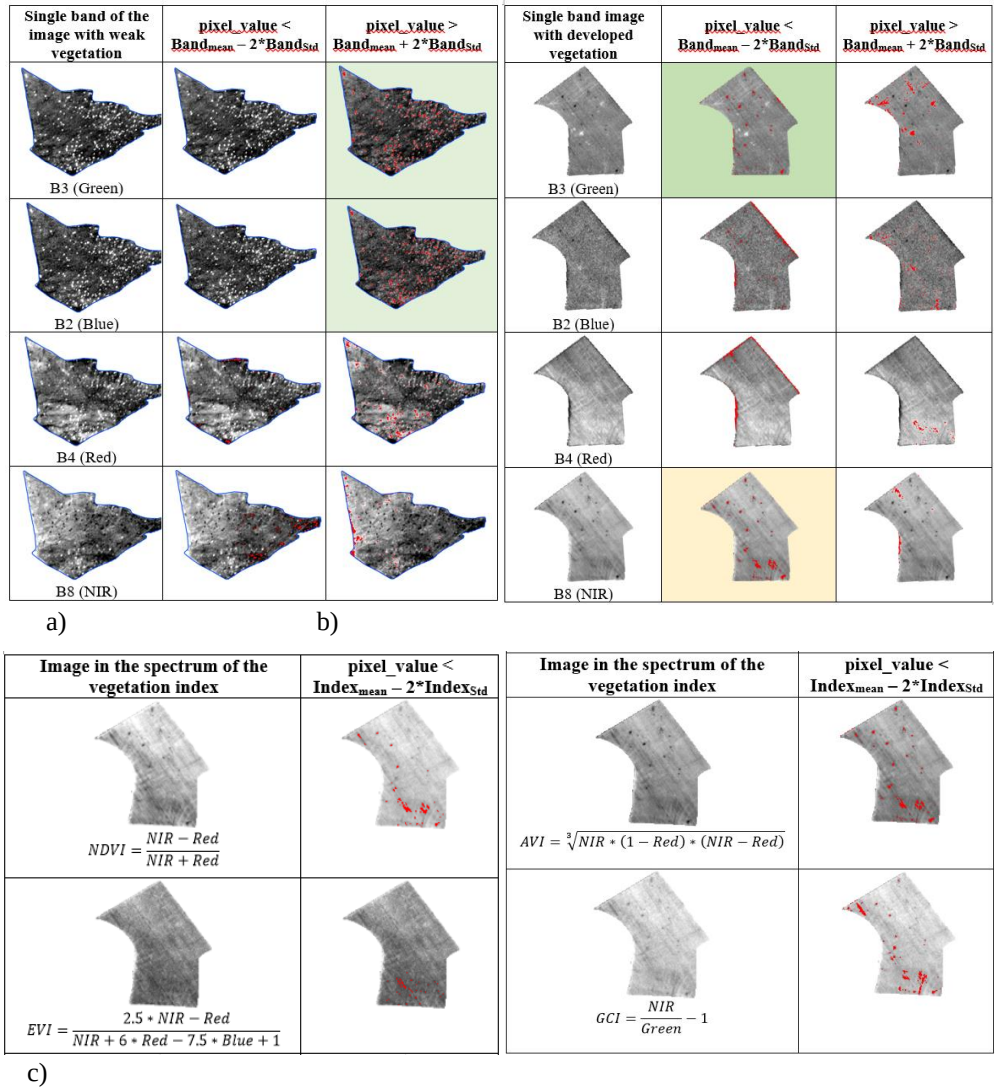

Fig. 5. Detection of anomalous pixels in fields:
a – spectral bands under low vegetation, b - spectral bands under high vegetation, c - vegetation indices under high vegetation

As seen from Fig. 5, the most informative bands for detecting damage on fields with low vegetation are bands B2 and B3, while on fields with high vegetation, bands B2, B8 (to a lesser extent), and vegetation indices NDVI, AVI, GCI are more informative.

Summarizing the results of both experiments (Fig. 4 and Fig. 5), we have identified that the most informative bands are B2, B3, and vegetation indices NDVI, GCI.

4.2. Classification for detecting damaged fields

Having selected the most informative bands (B2, B3) and vegetation indices (NDVI, GCI), we can use these data as input parameters for training a classifier to automatically recognize damaged fields.

The training dataset creation

To train the classifier, we first need a training dataset containing both damaged and undamaged field examples. To collect such data, three independent experts were engaged to sequentially review all fields in Sentinel-2 two-week composites from the beginning of the conflict until the end of 2022. Using satellite image-interpretation of satellite images, experts identified damages. Thus, from February 24, 2022, to December 31, 2022, experts identified approximately 13,211 damaged fields. From these fields, we form a subset to which we assign the label 1 (i.e., damaged field). To form a subset of undamaged fields (label 0), we use satellite images from 2021 for the same fields. That is, all fields identified as damaged by experts in 2022 are considered undamaged in 2021.

Classifier Architecture

For the classification task, we opted for a Random Forest Classifier (RF). Random Forest was chosen due to its good adaptation to a large number of features in satellite data [30], its ability to assess the importance of individual features, and successful experience in recognizing objects in images [31].

The model we selected is a binary classifier consisting of 10 decision trees without restrictions on the number of leaf nodes per tree. As input parameters for the classifier, we use pre-calculated statistical indicators within each field from the training dataset, including maximum, mean, minimum values, and variance of spectral bands B2, B3, and vegetation indices

NDVI, GCI. It is worth noting again that to compute these indicators for fields labeled as 1 (damaged fields), we use satellite data from 2022, and for fields with similar vector boundaries but labeled as 0 (undamaged), we use data from 2021.

For model evaluation, we employ user accuracy (recall, Formula 2), producer accuracy (precision, Formula 3), and f1-score (Formula 4).

$$User's\ accuracy = \frac{Tp}{Tp+Fp}, \tag{2}$$

$$Producer's\ accuracy = \frac{Tp}{Tp+Fn}, \tag{3}$$

$$f1\_score = \frac{2Tp}{2Tp+Fn+Fp} \tag{4}$$

To ensure the credibility of the experiment, considering vegetation changes, we construct separate classification models for each two-week period of the study. We employ a 5-fold cross-validation method (80% for training and 20% for validation). During this process, we evaluate accuracy metrics for each iteration and calculate their mean values, providing accuracy estimates for each period. Ultimately, we average these accuracy metrics across the periods to determine the overall classification.

4.3. Applying Anomaly Detection Method for Local Damage Identification

After conducting the classification, we obtain a vector map of damaged fields, allowing us to precisely determine the location of damages within each field. To achieve this, we apply an anomaly detection method to the spectral bands B2, B3, and vegetation indices NDVI, GCI. Relying solely on individual spectral bands or vegetation indices may lead to underestimation or overestimation of the actual damaged areas. To overcome these limitations and enhance the accuracy of damage detection, we propose combining vegetation index data with spectral bands.

Formula 1 enables the detection of anomalies in spectral bands. For identifying anomalies in vegetation indices, we propose another algorithm (Fig. 6). Specifically, we apply a 5x5 pixel averaging filter to raster maps of vegetation indices. Next, we compute the difference ($Index_{diff}$) between the actual vegetation index values ($Index_{real}$) and the smoothed values ($Index_{filter}$) for each pixel (Formula 5). This differential analysis helps identify anomalies or deviations, signaling potential field damage.

$$Index_{diff} = Index_{filter} - Index_{real}, \tag{5}$$

Following this, based on the obtained $Index_{diff}$ map, we calculate statistical indicators within each field, specifically the mean value and standard deviation. Thus, damaged pixels are determined by Formula 6:

$$Index_{damaged} = \begin{cases} 0, if\ Index_{diff} - k * (Index_{diff_{mean}} + Index_{diff_{stdDev}}) < 0 \\ 1, if\ Index_{diff} - k * (Index_{diff_{mean}} + Index_{diff_{stdDev}}) \geq 0 \end{cases} \tag{6}$$

In this formula $Index_{diff}$ – is the difference between the filtered (smoothed) and real values of the vegetation index, $Index_{diff_{mean}}$ – is the mean value of $Index_{diff}$ within the boundaries of the field, $Index_{diff_{stdDev}}$ – is the standard deviation of $Index_{diff}$ within the boundaries of the field, k – is a threshold coefficient, experimentally chosen (Table 1), $Index_{damaged}$ – is the anomalous values of the vegetation index within the field.

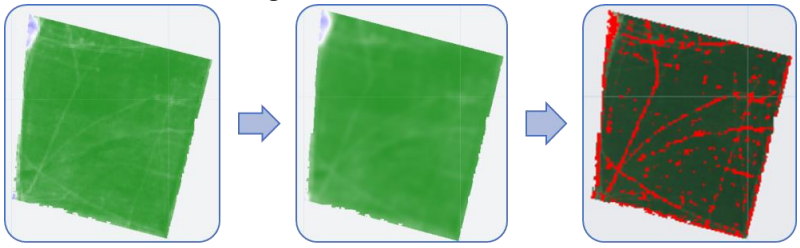

Real NDVI-image *Filtered NDVI-image* *Detected damages*

Fig. 6. Determining damage using vegetation indices per the filtering method

Table 1 - Threshold Coefficients for Damage Identification

Vegetation index or spectral band	Coefficient k
NDVI	0.5
GCI	1
GCI(1)	-0.7
B2	-0.7
B3	0.4

For the vegetation index GCI, we have defined two different coefficients, k, for fields with weak and strong vegetation. This differentiation helps identify different types of damage: the GCI index with a positive coefficient is sensitive to shallow craters (bright spots), while the GCI(1) index with a negative coefficient detects deeper craters (dark spots).

We have determined that simultaneous anomaly detection using NDVI and GCI (Fig. 7a) allows the identification of war-induced damages in fields with dense vegetation. The combination of band B3 and the inverse GCI index identifies craters in fields with moderate to low vegetation (Fig. 7b), as well as the combination of band B2 and the GCI (Fig. 7c).

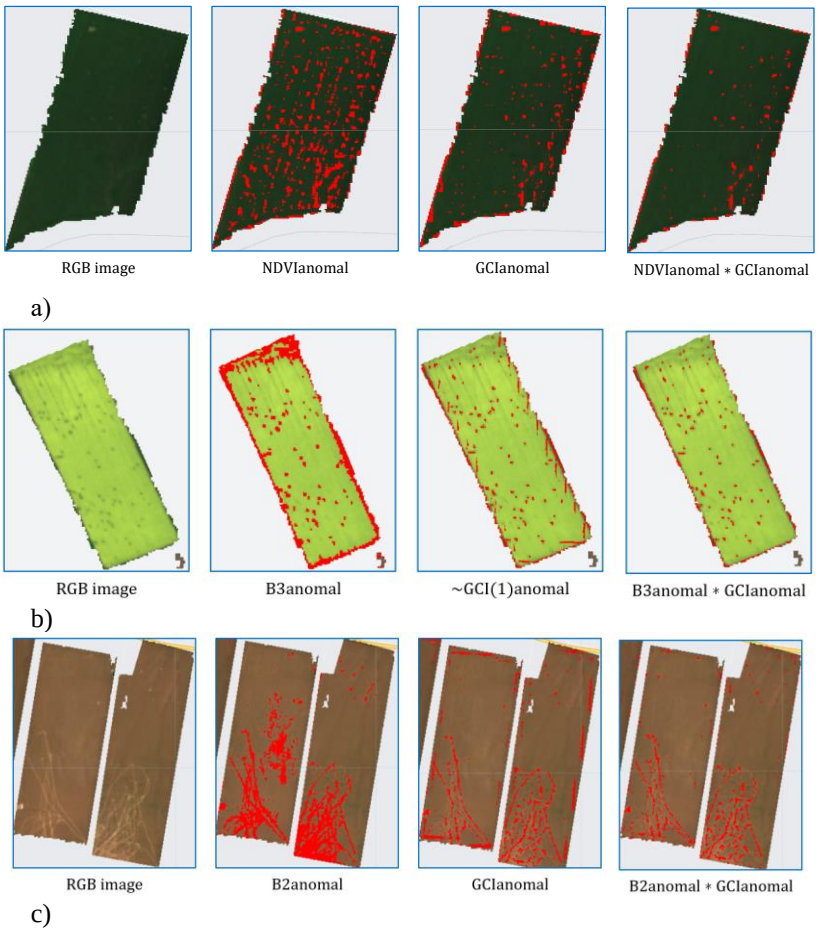

Fig. 7. Determining damage using the anomaly detection method: a - NDVI and GCI indices, (NDVI = 0.87>0.65), b - band B3 and inverse GCI index (NDVI=0.63<0.65), c - band B2 and GCI index (NDVI=0.43<0.65)

To encompass these three cases, we have devised a general formula 4:

$$Damaged = \begin{cases} NDVI_{anomal}\ and\ GCI_{anomal},\ if\ NDVI_{mean} \geq 0.65 \\ (B2_{anomal}\ and\ GCI_{anomal})\ or\ (\ GCI(1)_{anomal}\ and\ B3_{anomal}), if\ NDVI_{mean} < 0.65 \end{cases} \quad (4)$$

This formula is the main formula that we use to search for anomalies to identify local damages in fields.

5. Results

5.1. Classification Accuracy Assessment and Detection of Damaged Fields

The classification accuracy results for each bi-weekly period throughout 2022 are presented in Fig. 8a. As observed, the accuracy consistently maintains a high level, not dropping below 0.7 (6th period). Minor declines in accuracy are recorded in the 8th and 13th periods, possibly attributed to the inadequate quality of input data due to cloud cover.

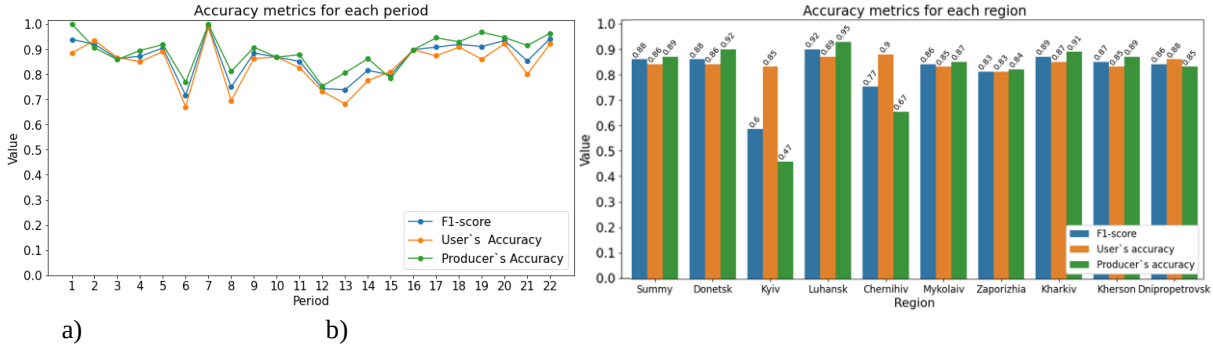

Fig. 8. Classification accuracy: a – by periods, b – by regions

For a better interpretation of accuracy metrics, we also calculated them separately for each of the regions. Fig. 8b illustrates a discrepancy in user and producer accuracy for the Kyiv and Chernihiv regions. This is attributed to the limited number of damaged fields, as active combat operations ceased in these regions starting from April 1.

The confusion matrix presented in Fig. 9 indicates that the average F1-score over the periods is 0.87, complemented by an average user accuracy of 0.89 and an average producer accuracy of 0.85. These metrics attest to the effectiveness of our methodology in identifying damaged fields.

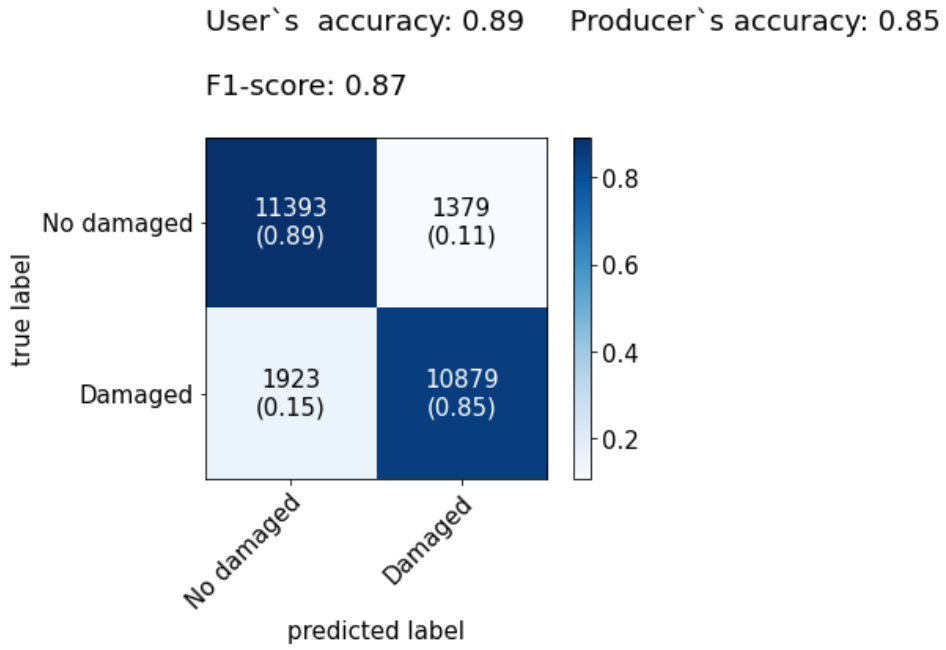

Fig. 9. Averaged confusion matrix

Using the developed classifier, we conducted a search for damaged fields in the research area from the beginning of the conflict until December 3, 2023, and aggregated the damaged areas over bi-weekly periods to determine when the agricultural sector was most severely affected by the hostilities. As evident from Fig. 10, the most damage to agricultural fields occurred during the 2nd (104,204 ha of damaged fields), 23rd (130,478 ha), and 25th (112,338 ha) periods of the conflict. It can be observed that in 2022, the intensity of damage was slightly higher than in 2023.

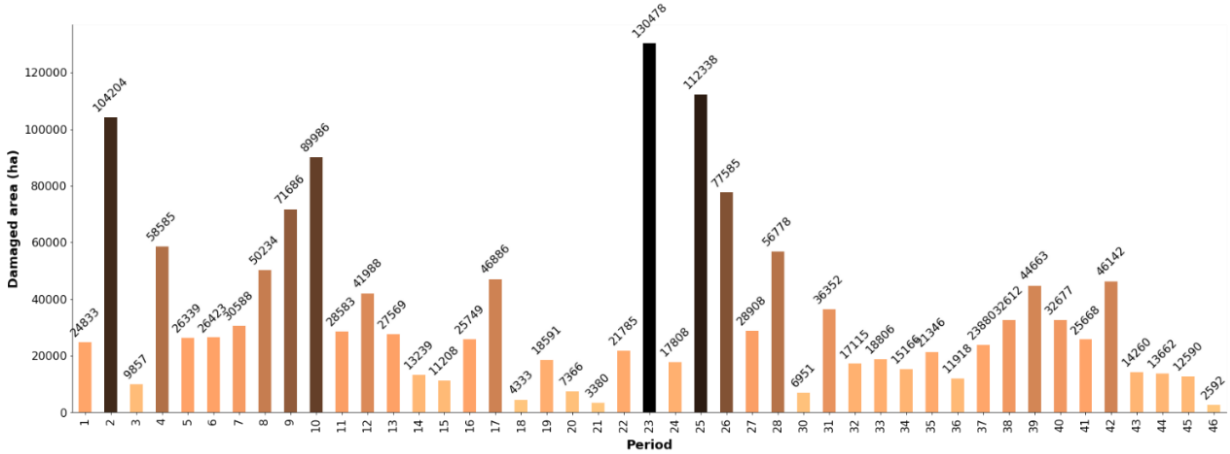

Fig. 10. Distribution of damaged areas by periods

To determine which regions are most affected, we aggregated the damaged areas by region. As seen in Fig. 11, the damaged territories are concentrated primarily on the border between the controlled territory of Ukraine and the occupied part of Russia, where active hostilities persist. According to the estimates, the most affected regions are Donetsk (378,449 ha), Zaporizhia (310,918 ha), and Kherson (290,329 ha).

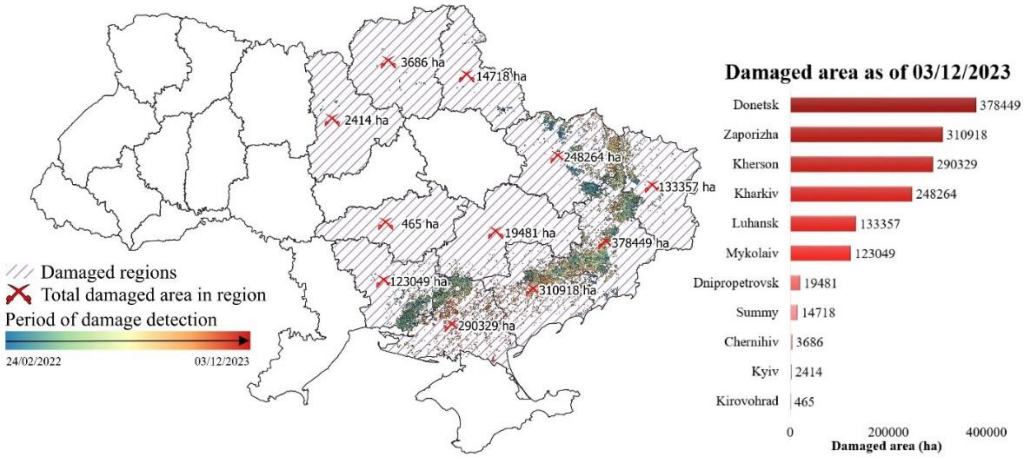

Fig. 11. Distribution of damaged areas by regions

Using the anomaly analysis method, we can identify craters and assess the severity of damage to the fields (Fig. 12). To check the sensitivity of the developed anomaly analysis method, we used a visual assessment. To do this, we selected a field on the border between Donetsk and Luhansk regions, for which commercial images were available on 07.02.2022 from the MAXAR satellite with a spatial resolution of 0.5m, and applied our method to Sentinel-2 images for the same date. As can be seen from Fig. 12, Sentinel-2 allows us to see mostly large craters due to its spatial resolution, but our anomaly analysis method detects all these craters. This confirms the effectiveness of the method.

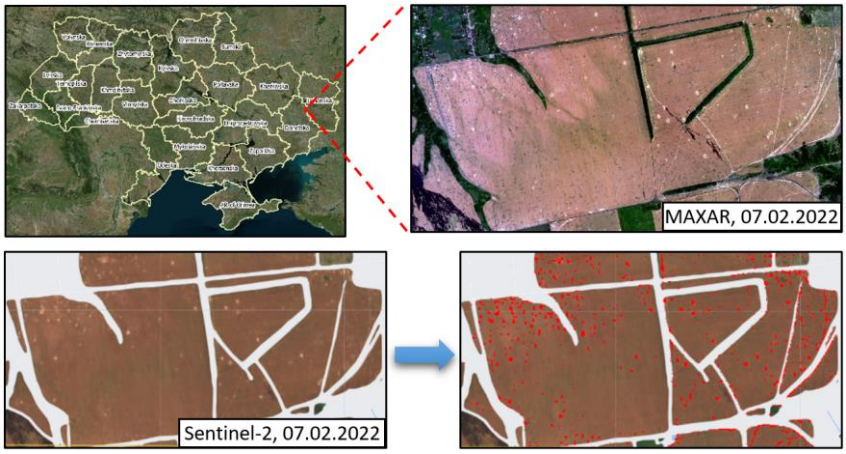

Fig. 12. Example of craters detection

Furthermore, we computed the damaged areas specific to various agricultural crops to evaluate the severity of the deficit for each crop in Ukraine. As depicted in Fig. 13, the most extensively affected are wheat fields, with 509,107 hectares damaged, constituting 4.1% in 2022 and 1.9% in 2023 of the overall wheat sown area. Sunflower fields follow, with 114,302 hectares affected, accounting for 0.5% in 2022 and 1% of the total sunflower sown area. Maize fields show damage on 68,830 hectares, representing 0.9% in 2022 and 0.5% in 2023 of the overall maize sown area. Similarly, rapeseed fields suffered damage on 46,029 hectares, making up 2.2% in 2022 and 0.6% in 2023 of the total rapeseed sown area. Additionally, non-cultivated fields covering 165,761 hectares were affected.

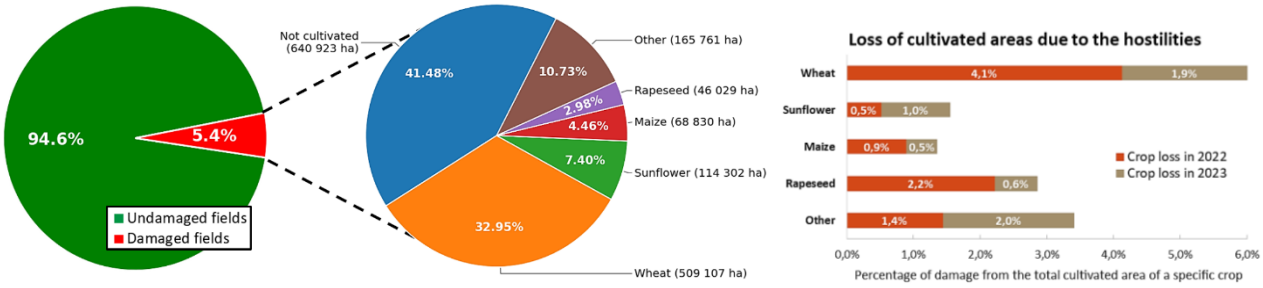

a) b)

Fig. 13. Loss of cultivated areas:
a - distribution of damaged areas by crops, b - percentage of damaged cultivated land of the total cultivated area for a specific crop (2022-2023)

As a result, from the beginning of the war to the end of 2023, about 1,544,952 hectares of agricultural fields were damaged, which is equivalent to 5.72% of all agricultural land in Ukraine.

6. Conclusion

This study developed and applied a method for automatic detection of war-damaged agricultural fields and recognition of local damages using machine learning and anomaly detection based on free Sentinel-2 satellite imagery. Spectral bands B2, B3, and vegetation indices NDVI, GCI proved to be the most informative for identifying damages to agricultural fields.

The developed random forest classifier algorithm demonstrated high accuracy and effectiveness with an average f1-score of 0.87, precision of 0.85, and recall of 0.89. Classification errors were attributed to insufficient or low-quality training data due to cloud cover in the images.

The anomaly analysis method accurately determines the location and size of craters, traces of military vehicle movement, etc., on classified fields. This method allows for assessing the degree of damage to a specific field, identifying landowners in greatest need of assistance. Among the limitations of the method is sensitivity to anomalies caused not only by war activities, requiring careful selection of the threshold coefficient.

A comprehensive analysis of the results revealed that from the beginning of the war to December 3, 2023, 1,544,952 hectares of fields in Ukraine were damaged (5.72% of all agricultural lands), including 41.48% non-cultivated fields, 32.95% wheat fields, 7.4% corn fields, 4.46% sunflower fields, 2.98% rapeseed fields, and 10.73% other crops. The most damaged regions are Donetsk, Zaporizhzhia, Kherson, Kharkiv, and Luhansk regions.

The obtained results hold significant practical importance for the Ukrainian government and international organizations, aiding in effectively planning resources for the restoration of damaged fields and infrastructure in Ukraine.

7. References

1. Glauber, J. W., & Laborde, D. (2023). Regional war, global consequences: Mounting damages to Ukraine's agriculture and growing challenges for global food security. *IFPRI book chapters*, 120-124. https://doi.org/10.2499/9780896294394_23

2. Deininger, K., Ali, D. A., Kussul, N., Shelestov, A., Lemoine, G., & Yailimova, H. (2023). Quantifying war-induced crop losses in Ukraine in near real time to strengthen local and global food security. *Food Policy*, *115*, 102418. https://doi.org/10.1016/j.foodpol.2023.102418

3. Agricultural War Damages, Losses, and Needs Review Issue 3 April 24, 2023. (2023). In *kse.ua*. Kyiv School of Economics. Retrieved January 18, 2024, from https://kse.ua/wp-content/uploads/2023/05/RDNA2.pdf

4. Shelestov, A., Shumilo, L., Yailymova, H., & Drozd, S. (2021, November). Crop Yield Forecasting for Major Crops in Ukraine. In *2021 IEEE International Conference on Information and (UkrMiCo)* (pp. 35-38). IEEE. https://doi.org/10.1109/UkrMiCo52950.2021.9716672

5. Shumilo, L., Drozd, S., Kussul, N., Shelestov, A., & Sylantyev, S. (2021, April). Mathematical Models and Informational Technologies of Crop Yield Forecasting in Cloud Environment. In *International Scientific and Technical Conference-Modern Challenges in Telecommunications* (pp. 143-164). Cham: Springer International Publishing. https://doi.org/10.1007/978-3-031-16368-5_7

6. Kussul, N., Drozd, S., & Yailymova, H. (2023, March). Forecast of Yield of Major Crops in Ukraine in War Conditions 2022 Based on MODIS and Sentinel-2 Satellite Data. In *Proceedings of International Conference on Applied Innovation in IT* (Vol. 11, No. 1, pp. 89-95). Anhalt University of Applied Sciences. https://doi.org/10.25673/101923

7. Skakun, S., Kussul, N., Shelestov, A., & Kussul, O. (2016). The use of satellite data for agriculture drought risk quantification in Ukraine. *Geomatics, Natural Hazards and Risk*, *7*(3), 901-917. https://doi.org/10.1080/19475705.2015.1016555

8. Bayissa, Y. A., Tadesse, T., Svoboda, M., Wardlow, B., Poulsen, C., Swigart, J., & Van Andel, S. J. (2019). Developing a satellite-based combined drought indicator to monitor agricultural drought: A case study for Ethiopia. *GIScience & Remote Sensing*, *56*(5), 718-748. https://doi.org/10.1080/15481603.2018.1552508

9. Baek, S. G., Jang, H. W., Kim, J. S., & Lee, J. H. (2016). Agricultural drought monitoring using the satellite-based vegetation index. *Journal of Korea Water Resources Association*, *49*(4), 305-314. https://doi.org/10.1088/1757-899X/732/1/012063

10. Tapia-Silva, F. O., Itzerott, S., Foerster, S., Kuhlmann, B., & Kreibich, H. (2011). Estimation of flood losses to agricultural crops using remote sensing. *Physics and Chemistry of the Earth, Parts A/B/C*, *36*(7-8), 253-265. https://doi.org/10.1016/j.pce.2011.03.005

11. Bell, J. R., & Molthan, A. L. (2016). Evaluation of Approaches to Identifying Hail Damage to Crop Vegetation Using Satellite Imagery. *Journal of Operational Meteorology*, *4*(11). http://dx.doi.org/10.15191/nwajom.2016.0411

12. Prabhakar, M., Gopinath, K. A., Reddy, A. G. K., Thirupathi, M., & Rao, C. S. (2019). Mapping hailstorm damaged crop area using multispectral satellite data. *The Egyptian Journal of Remote Sensing and Space Science*, *22*(1), 73-79. https://doi.org/10.1016/j.ejrs.2018.09.001

13. Lin, E., Qin, R., Edgerton, J., & Kong, D. (2020). Crater detection from commercial satellite imagery to estimate unexploded ordnance in Cambodian agricultural land. *Plos one*, *15*(3), e0229826. https://doi.org/10.1371/journal.pone.0229826

14. Kussul, N., Shumilo, L., Yailymova, H., Shelestov, A., & Krasilnikova, T. (2023). Complex method for land degradation estimation. In *IOP Conference Series: Earth and Environmental Science* (Vol. 1126, No. 1, p. 012032). IOP Publishing. https://doi.org/10.1088/1755-1315/1126/1/012032

15. Kussul, N., Fedorov, O., Yailymov, B., Pidgorodetska, L., Kolos, L., Yailymova, H., & Shelestov, A. (2023). Fire danger assessment using moderate-spatial resolution satellite data. *Fire*, *6*(2), 72. https://doi.org/10.3390/fire6020072

16. Shumilo, L., Yailymov, B., & Shelestov, A. (2020, September). Active fire monitoring service for Ukraine based on satellite data. In *IGARSS 2020-2020 IEEE International Geoscience and Remote Sensing Symposium* (pp. 2913-2916). IEEE. https://doi.org/10.1109/IGARSS39084.2020.9323922.

17. Kussul, N., Yailymova, H., & Drozd, S. (2022, December). Detection of War-Damaged Agricultural Fields of Ukraine Based on Vegetation Indices Using Sentinel-2 Data. In *2022 12th International Conference on Dependable Systems, Services and Technologies (DESSERT)* (pp. 1-5). IEEE. https://doi.org/10.1109/DESSERT58054.2022.10018739

18. Shelestov, A., Drozd, S., Mikava, P., Barabash, I., & Yailymova, H. (2023, March). War Damage Detection Based on Satellite Data. In *Proceedings of International Conference on Applied Innovation in IT* (Vol. 11, No. 1, pp. 97-103). Anhalt University of Applied Sciences. https://doi.org/10.25673/101924

19. Witmer, F. D. (2008). Detecting war-induced abandoned agricultural land in northeast Bosnia using multispectral, multitemporal Landsat TM imagery. *International Journal of Remote Sensing*, *29*(13), 3805-3831. https://doi.org/10.1080/01431160801891879

20. Gibson, G. R. (2012). *War and agriculture: three decades of agricultural land use and land cover change in Iraq* (Doctoral dissertation, Virginia Tech). http://hdl.handle.net/10919/27671

21. Eklund, L., Degerald, M., Brandt, M., Prishchepov, A. V., & Pilesjö, P. (2017). How conflict affects land use: agricultural activity in areas seized by the Islamic State. *Environmental Research Letters*, *12*(5), 054004. https://doi.org/10.1088/1748-9326/aa673a

22. Kostyuchenko, Y. V., Yuschenko, M., Movchan, D., & Kopachevsky, I. (2017, October). Analysis of economic values of land use and land cover changes in crisis territories by satellite data: models of socio-economy and population dynamics in war. In *Earth Resources and Environmental Remote Sensing/GIS Applications VIII* (Vol. 10428, pp. 110-126). SPIE. https://doi.org/10.1117/12.2276153

23. Skakun, S., Justice, C. O., Kussul, N., Shelestov, A., & Lavreniuk, M. (2019). Satellite data reveal cropland losses in South-Eastern Ukraine under military conflict. *Frontiers in Earth Science*, 305. https://doi.org/10.3389/feart.2019.0

24. Lacroix, V., & Vanhuysse, S. (2015, January). Crater Detection using CGC. In *Proceedings of the International Conference on Pattern Recognition Applications and Methods-Volume 1* (pp. 320-327). https://doi.org/10.5220/0005222503200327

25. Duncan, E. C., Skakun, S., Kariryaa, A., & Prishchepov, A. V. (2023). Detection and mapping of artillery craters with very high spatial resolution satellite imagery and deep learning. *Science of Remote Sensing*, *7*, 100092. https://doi.org/10.1016/j.srs.2023.100092

26. About ACLED. ACLED. (2023, December 5). https://acleddata.com/about-acled/

27. Ministry of Agrarian Policy and Food of Ukraine. (2023). *Crop map of Ukraine 2022*. Ukraine-cropmaps. https://ukraine-cropmaps.com/

28. Kuzin, V., Musial, J., & Shelestov, A. (2022, December). EO4UA Initiative: Scientific European Support of Ukrainian Scientific Community. In *2022 12th International Conference on Dependable Systems, Services and Technologies (DESSERT)* (pp. 1-5). IEEE. https://doi.org/10.1109/DESSERT58054.2022.10018706.

29. Livingston, E. H. (2004). The mean and standard deviation: what does it all mean?. *Journal of Surgical Research*, *119*(2), 117-123. https://doi.org/10.1016/j.jss.2004.02.008

30. Pelletier, C., Valero, S., Inglada, J., Champion, N., & Dedieu, G. (2016). Assessing the robustness of Random Forests to map land cover with high resolution satellite image time series over large areas. *Remote Sensing of Environment*, *187*, 156-168. https://doi.org/10.1016/j.rse.2016.10.010

31. Payet, N., & Todorovic, S. (2013). Hough forest random field for object recognition and segmentation. *IEEE transactions on pattern analysis and machine intelligence*, *35*(5), 1066–1079. https://doi.org/10.1109/TPAMI.2012.194